

General Disclaimer

One or more of the Following Statements may affect this Document

- This document has been reproduced from the best copy furnished by the organizational source. It is being released in the interest of making available as much information as possible.
- This document may contain data, which exceeds the sheet parameters. It was furnished in this condition by the organizational source and is the best copy available.
- This document may contain tone-on-tone or color graphs, charts and/or pictures, which have been reproduced in black and white.
- This document is paginated as submitted by the original source.
- Portions of this document are not fully legible due to the historical nature of some of the material. However, it is the best reproduction available from the original submission.

X-621-68-449

~~PREPRINT~~

(Revised 1/15/69)

NASA TM X-~~63408~~ 63408

A TWO DIMENSIONAL MODEL
OF THE DIURNAL VARIATION
OF THE THERMOSPHERE

F-72192

H. VOLAND
H.G. MAYR
W. PRIESTER



NOVEMBER 1968

GSFC

— GODDARD SPACE FLIGHT CENTER —
GREENBELT, MARYLAND

FACILITY FORM 602

N 69-18109

(ACCESSION NUMBER)

42

(THRU)

1

(PAGES)

TMX-63408

(CODE)

13

(NASA CR OR TMX OR AD NUMBER)

(CATEGORY)

X-621-68-449
Preprint

A TWO DIMENSIONAL MODEL OF THE
DIURNAL VARIATION OF THE THERMOSPHERE

PART II

AN EXPLANATION OF THE "SECOND HEAT SOURCE"

H. Volland*, H. G. Mayr and W. Priester*

*On leave from the Astronomical Institutes of the University of Bonn, Germany,
as a NAS-NRC Research Associate.

GODDARD SPACE FLIGHT CENTER
Greenbelt, Maryland

LEADING PAGE BLANK NOT FILMED.

A TWO DIMENSIONAL MODEL OF THE
DIURNAL VARIATION OF THE THERMOSPHERE

PART II

AN EXPLANATION OF THE "SECOND HEAT SOURCE"

H. Volland, H. G. Mayr and W. Priester

ABSTRACT

A two dimensional model of the thermosphere between 120 and 400 km is presented in which solar EUV heat input is the only external heat source taken into account. By choosing the boundary values of the model appropriately, amplitude and phase of the observed diurnal variations of density, temperature and winds are reproduced in a consistent manner. It is concluded that horizontal convection, convective energy coupling between lower atmosphere and thermosphere and heat conductive energy exchange between thermosphere and exosphere are of great significance for the energy and particle balance of the thermosphere. These processes were basically neglected in Harris and Priester's model. Therefore they must be considered to be the origin of their "second heat source".

A TWO DIMENSIONAL MODEL OF THE DIURNAL VARIATION OF THE THERMOSPHERE

PART II

AN EXPLANATION OF THE "SECOND HEAT SOURCE"

1. INTRODUCTION

The first theoretical model of the diurnal behavior of the thermosphere was one dimensional [Harris and Priester (1962)]. Dealing exclusively with solar EUV as diurnal heat source, their numerical results gave too high density variations as compared with observations and their density maximum appeared at 17° local time, which is in contrast to observations showing a maximum at 14° local time. Harris and Priester therefore introduced an ad hoc "second heat source" which was provided in such a way that it could supplement the solar EUV heat source and bring agreement between calculations and measurements. They assumed as boundary conditions zero variation of pressure, temperature and vertical wind at the lower level (120 km) and zero variation of the temperature gradient at the top of their model at 800 km height. This choice of boundary conditions limited the wave energy exchange to heat convection at the upper boundary and to heat conduction at the lower boundary. These assumptions were extremely convenient for the calculations and they appeared to be rather plausible at that time. Yet they are in fact completely arbitrary and unjustified, and as it will be shown in this paper, they constitute unrealistic restrictions.

In a later paper Harris and Priester (1965) tried to overcome some of these restrictions by allowing finite temperature and pressure variations at the lower boundary of their model. Yet even this did not replace the need for the "second heat source".

In an earlier paper (Volland, 1966) (referred to as paper I) the thermosphere was treated by a two dimensional model. In this paper the basic equations for the dynamical behavior of the diurnal variations within a two dimensional thermosphere as well as approximate analytical solutions were given. This model is valid during the time of equinox and at low latitudes. Thus latitudinal winds have been excluded and only longitudinal and vertical winds within the equatorial plane have been considered. In paper I it was proposed that horizontal and (or) vertical winds could replace the "second heat source" which was required in Harris and Priester's one dimensional model. These winds could transport heat energy through convection and therefore should be able to shift the density maximum into the early afternoon which is in agreement with observations. In a second paper (Volland 1967) this idea was qualitatively confirmed. In addition to horizontal heat convection a finite vertical temperature gradient at the upper boundary of the model was introduced to shift the phase of the density and temperature into the desired direction. However quantitative agreement with observations still could not be achieved. Again, the failure to reproduce the observations must be attributed to the restraining choice of boundary conditions. Although allowing conductive and convective energy exchange at the upper boundary this model isolated the thermosphere entirely from the atmosphere below by assuming the variations of temperature gradient and vertical velocity to be zero at the lower level.

Recently Dickinson et al. (1968) calculated a two dimensional model of the thermosphere taking into account only the solar EUV heat source. In order to obtain realistic results and agreement with observations they had to introduce another form of "second heat source"—in this case an artificial reduction of their wind velocity by an arbitrary "scale factor" which was thought to compensate the neglect of ion drag and viscosity. It can in fact be shown (Volland, 1969b) that ion drag has a significant influence for the phase of the density variations. In addition to that however the failure to obtain self consistent results is also due to the unrealistic boundary conditions which were in this case zero vertical velocity at the bottom and zero variation of the temperature gradient at the top and the bottom of their model.

There are several reasons why the fixed boundary conditions, employed in the above models, are unrealistic. Zero variation of pressure and vertical velocity at the lower boundary implies that convective energy coupling between the lower and upper atmosphere is excluded. But we know from observations of the geomagnetic S_q current that a horizontal wind system with velocities of the order of 50 m/sec must exist between 100 and 120 km altitude (Kato, 1956). Such a wind system is necessarily accompanied by vertical winds and temperature and pressure variations. Rocket borne measurements of the N_2 density at heights between 150 and 300 km by Spencer et al. (1966) and Taeusch et al. (1968) have indeed revealed variations in the lower thermosphere which are much larger than those predicted in the Harris and Priester model (CIRA, 1965) or Jacchia's model (Jacchia, 1964). Therefore we must expect—and our calculations will confirm this—that the convective energy exchange between the lower and upper atmosphere significantly influences the density and temperature structure of the thermosphere.

At the upper boundary of the Harris and Priester model as well as in the Dickinson et al. model the zero variation of the temperature gradient they enforce suppresses heat conduction and permits wave energy exchange through the upper boundary to occur only by heat convection. In view of the increasing significance of heat conduction at higher altitudes this assumption is unjustified. Furthermore, the over emphasis on heat convection enhances the mass transport through this boundary and therefore can be attributed to the resulting too high theoretical density variation at high altitudes that is also in disagreement with observations.

We shall show in this paper that without physically unacceptable restrictions on the boundary conditions a self consistent solution can be obtained that is in good agreement with basic observational data between 120 and 400 km. Thereby, solar EUV heat input is shown to be entirely sufficient as an external source. It will be seen that a combination of horizontal and vertical heat convection within the lower thermosphere and a combination of horizontal heat convection and vertical heat conduction within the upper part of the thermosphere constitute the "second heat source". Heat convection within the lower thermosphere is maintained mainly by a tidal gravity wave penetrating from below into the thermosphere, which is consistent with a prediction of Lindzen (1967).

2. THE MODEL

The theory presented in paper I describes a two dimensional thermosphere model valid at low latitudes and during equinox. We shall use this theory with the following restrictions.

a.) Perturbation Theory. A time average thermosphere model derived from Model 4 of CIRA (1965) is adopted for density, temperature and mean molecular mass. Perturbation theory is applied; thus only the first harmonics of the diurnal variations are treated and all squares and higher order terms of the diurnal wave parameters are neglected. It has been shown by Volland (1967) that nonlinear terms affect the results in two ways. First, they transfer energy from the time dependent system into the time independent system. Since we shall use a given time independent system from CIRA (1965) we implicitly cannot account for this effect but rather we must add it to the uncertainties in the CIRA model. Second, the nonlinear terms prevent an unlimited increase of the perturbation amplitude which in our case is only accomplished by wave energy dissipation due to heat conduction. As long as the relative wave amplitudes are smaller than 0.3 in magnitude it turns out that perturbation theory is a sufficient approximation. This will generally hold for altitudes lower than 400 km, which is the reason why we had to choose this level as upper boundary. If the relative wave amplitudes are larger than 0.3 they have to be considered only as upper limits.

b.) External Heat Input. As external heat source the diurnal EUV heat input was taken from CIRA model 4, thus, it is independent of the resulting density distribution. This greatly simplifies the numerical calculations. In view of the large uncertainties about the efficiency factor of the solar heat input, the assumption of a given EUV source does not add much to the uncertainties already involved in the problem.

c.) Molecular Viscosity. Molecular viscosity is neglected which also greatly simplifies the calculations because under these circumstances only 4 characteristic waves (two gravity waves and two heat conduction waves) remain and an analytical solution of their eigenvalues exists (Volland, 1969). Viscosity can be neglected if the Reynolds number

$$R = \left| \frac{\rho \frac{\partial v}{\partial t}}{\eta \left(\frac{\partial^2 v}{\partial y^2} + \frac{\partial^2 v}{\partial z^2} \right)} \right| \gg 1 \quad (1)$$

greatly exceeds unity. v is the horizontal velocity, ρ is the mean density, t is the time, y the longitude, z the altitude and η is the coefficient of molecular viscosity. Our calculations show that the Equation (1) holds throughout the thermosphere below 400 km.

3. SOLUTION OF THE DYNAMICS OF THE THERMOSPHERE

Because of the restrictions mentioned in section 2, the system of equations describing the dynamic behavior of the thermosphere is a set of four complex coupled ordinary linear differential equations of first order which we write in concise matrix form [see Equation (10) in paper I]

$$\frac{d \mathbf{e}}{dz} = jk \left(\mathbf{K}(z) \mathbf{e} + \mathbf{h}(z) \right) \quad (2)$$

where \mathbf{e} and \mathbf{h} are column matrices containing the elements

$$e_1 = \sqrt{C_p} \frac{\Delta w}{C}$$

$$e_2 = \sqrt{C_p} \frac{\Delta p}{p}$$

$$e_3 = \sqrt{C_p} \frac{\Delta T}{T}$$

$$e_4 = \sqrt{C_p} \frac{\kappa (d \Delta T / dz)}{C_p}$$

$$h_1 = h_2 = h_3 = 0$$

$$h_4 = j \frac{\Delta Q_{EUV}}{\omega} \sqrt{\frac{C}{p}}$$

and the 4×4 - coefficient matrix K depending on height z can be found in [Volland, 1969, Equation (43)].

It is

$$\left. \begin{array}{c} \Delta w \\ \Delta p \\ \Delta T \\ \Delta \rho \\ \Delta v \end{array} \right\} \text{wave amplitudes of} \quad \left. \begin{array}{c} \text{vertical wind velocity} \\ \text{pressure} \\ \text{temperature} \\ \text{density} \\ \text{horizontal wind velocity} \end{array} \right\}$$

$$\left. \begin{array}{c} C \\ p \\ T \\ \rho \end{array} \right\} \text{height dependent mean values of} \quad \left. \begin{array}{c} \text{velocity of sound} \\ \text{pressure} \\ \text{temperature} \\ \text{density} \end{array} \right\}$$

Density and horizontal wind of the wave do not occur explicitly within Equations (2), but are linearly related with e_1 , e_2 and e_3 by the following expressions

$$\sqrt{C p} \frac{\Delta \rho}{\rho} = e_2 - e_3 \quad (3)$$

$$\sqrt{C p} \frac{\Delta v}{C} = \frac{1}{1 - j Z_2} \left(j Z_1 e_1 - \frac{S}{\gamma} e_2 \right)$$

ω is the angular frequency of the diurnal variation

$k = \frac{\omega}{C}$ is a normalizing wave number

κ is the coefficient of heat conductivity

ΔQ_{EUV} is the diurnal component of the solar EUV heat input

$Z_1 = 2$ is the Coriolis parameter

$Z_2 = \frac{\nu}{\omega}$ is a collision parameter

ν is the collision number between the ions and one neutral

γ is the ratio between the specific heats at constant pressure and constant volume

$S = \frac{k_y}{k}$ is a normalized horizontal wavenumber

$k_y = \frac{1}{a}$ is the horizontal wavenumber of the diurnal variation

a is the earth radius.

Four characteristic waves — two gravity waves and two heat conduction waves — can propagate within a homogeneous thermosphere in which heat conductivity is taken into account. Their vertical propagation characteristics are described by the formula

$$\mathbf{c} = \mathbf{\tilde{c}} e^{jkNz}$$

where the column matrix \mathbf{c} contains the four wave modes and

$$N = \begin{pmatrix} -q_1 & 0 & 0 & 0 \\ 0 & -q_2 & 0 & 0 \\ 0 & 0 & q_1 & 0 \\ 0 & 0 & 0 & q_2 \end{pmatrix} \quad (4)$$

is a diagonal matrix with the eigenvalues q_i of the matrix K as its elements. $\pm q_1$ are the two eigenvalues of up- and downgoing gravity waves, $\pm q_2$ are the two eigenvalues of up- and downgoing heat conduction waves given in Equation (44) in (Volland, 1969).

The characteristic waves are related with the physical parameters e of Equation (2) by

$$e = Q c \quad (5)$$

where Q can be found from the condition

$$K Q = Q N. \quad (6)$$

The characteristic waves c_i are normalized in such a manner that

$$c_i c_i^* = \frac{1}{2} \text{Real}(\Delta w_i \Delta p_i^*) \quad (7)$$

gives the time averaged vertical energy flux of the i th wave. (The star indicates conjugate complex values.)

If we divide the realistic atmosphere into a number of homogeneous isothermal slabs of thickness Δz_ℓ . Equations (2) to (6) lead in a straightforward manner to the solution

$$c(z_0) = P_0^n c(z_n) + r_0^n \quad (8)$$

with

$$P_i^s = \prod_{\ell=i+1}^s Q_{\ell-1}^{-1} \Gamma_\ell Q_\ell e^{-jk_\ell N_\ell \Delta z_\ell}$$

$$r_i^s = \sum_{\ell=i+1}^s P_\ell^s N_\ell^{-1} \left(E - e^{jk_\ell N_\ell \Delta z_\ell} \right) Q_\ell^{-1} h_\ell$$

$$\Gamma_\ell = \sqrt{\frac{C_{\ell-1}}{C_\ell}}$$

$C_\ell/C_{\ell-1}$	0	0	0
0	1	0	0
0	0	$T_\ell/T_{\ell-1}$	0
0	0	0	$C_\ell/C_{\ell-1}$

The matrix Γ_l matches the internal boundary conditions of continuous amplitudes of Δw , Δp , ΔT and $\kappa d(\Delta T)/dz$ between two slabs of temperatures T_{l-1} and T_l . E is a unit matrix.

The solution in the form of an analytical expression Equation (8) has the advantage that only once an integration has to be performed in order to determine the altitude depending functions $P_i^n(z_i)$ and $r_i^n(z_i)$. The rest — namely the selection of appropriate boundary conditions and the calculation of the physical parameters versus height via the transformation Equation (5) — is only a matter of solving four complex linear equations with four unknowns. The four unknowns are e.g. the characteristic waves $c(z_n)$ at the upper boundary.

In order to solve Equation (8) uniquely we need four complex or eight real boundary values for which we can choose either characteristic waves or physical parameters. In our calculations we apply the radiation condition which demands that waves generated within the thermosphere can only leave the boundaries of the thermosphere. Our boundary problem therefore reduces to one complex parameter — namely magnitude and phase of an upgoing tidal gravity wave from the lower atmosphere which must be chosen such that the calculations fit with the observations (Volland and Mayr, 1969).

4. NUMERICAL RESULTS OF THE DIURNALLY VARYING PHYSICAL PARAMETERS

As boundaries for our model we chose $z_0 = 120$ km and $z_n = 400$ km.

The measurements we shall compare our results with were made during moderate solar activity ($F = 100 - 150$). For this reason we adopt as input

the time average thermosphere components of density, temperature and molecular mass from model 4 of CIRA (1965).

In calculating the ion-neutral drag force we assumed that the ions are "frozen" into the magnetic field and thus the ion velocity component perpendicular to the magnetic field is zero. We employed Dalgarno's (1964) collision frequency

$$\nu = 7 \times 10^{-10} N_i \quad (\text{sec}^{-1}), \quad (9)$$

where N_i (in cm^{-3}) is the number density of ions. For N_i we assumed a value of 5×10^4 at 120 km and an exponential like increase with a scale height of 100 km.

As discussed in the previous section as boundary condition only one complex parameter is free to adjust the calculations to the observed data of temperature, density and winds (Volland and Mayr, 1969). This parameter was chosen as the complex wave parameter of the upward propagating gravity wave. Thus the solution of Equation (2) for e_i is uniquely determined.

If a_i are the time average parameters of pressure, temperature and density and Δa_i are the first (complex) harmonics of their diurnal variation, then the relation

$$\frac{\Delta a_i}{a_i} = \frac{1}{\sqrt{C_p}} e_i$$

is valid (according to section 3). In real representation the diurnal variation of the relative wave parameters ($\Delta a_i/a_i$) has the form

$$2 \operatorname{Real} \left\{ \frac{\Delta a_i}{a_i} e^{j\omega t} \right\} = A_i \cos [\omega(t - \tau_i)] \quad (10)$$

where

$$A_i = 2 \frac{|\Delta a_i|}{a_i} \quad (11)$$

is the relative magnitude and

$$\tau_i = -\frac{\arg(\Delta a_i)}{\omega} \quad (12)$$

is the time delay related to local midnight which gives the local time of the maximum of the parameters.

For the wind system in which the average velocities are zero, the absolute magnitudes

$$A_v = 2 |\Delta v|; A_w = 2 |\Delta w| .$$

are considered .

Our theory considers only the first Fourier component of the diurnal wave. Therefore we chose also the first Fourier component of the experimental data. Some of the observed data we compare our theory with do not allow a harmonic analysis because not enough data are available within a diurnal period. We therefore made use of another parameter, the ratio, f , between the observed maximum and minimum diurnal values, which is related to the relative magnitude A_i by the expression

$$f_i = \left(\frac{a_{\max}}{a_{\min}} \right)_i \sim \frac{1 + A_i}{1 - A_i} . \quad (13)$$

This relationship between f_i and A_i becomes exact if the observational data feature genuine diurnal harmonic variations.

Table I contains a list of authors and their observations which have been used for comparison with our calculations in Figures 1 to 4. Here, the CIRA model (No. I) requires a harmonic analysis, while the data of Kato (No. VI) give already the first Fourier component. The static model of Jacchia (No. II) does not permit the determination of the phase, and therefore only f -values can be derived. Likewise, from the observations No. III to VI only the parameters f_i can be determined.

Spencer et al. (1966) (No. III) and Taeusch et al. (1968) (No. IV) obtained the N_2 number density from a series of rocket flights on a single day. A comparison with our density values is only possible below about 200 km where N_2 is the major constituent. The temperature of N_2 , also measured by Spencer and Taeusch, is considered to be equal to the total gas temperature. The N_2 variations of Taeusch at 150 km altitude contain a semidiurnal component, which might affect the f -value. Therefore, we must consider this f -value with caution. The satellite drag observations by King-Hele and Hingston (1967), (1968) (No. V) have been derived from satellites with low perigee. For the height of 155 km King-Hele and Hingston (1967) give a value of $f_\rho = 1.7$ and a time delay of $\tau_\rho = 12^{\circ\circ}$. Considering only the first harmonic in their data we find the values of $f_\rho = 1.4$ and $\tau_\rho = 15^{\circ\circ}$. These values have been plotted in Figure 1. For the height of 190 km King-Hele and Hingston (1968) give the value $f_\rho = 1.4$ but no value of τ_ρ . They only state that the maximum density has been observed at day time. Therefore the phase of this observation has not been plotted in Figure 1b.

Mahajan's (1968) derived the ion temperature from Thomson backscatter spectra at Aricibo Ionospheric Observatory. The ion temperature is calculated to be up to 25°K higher than the neutral temperature at day time and at 250 km height while at nighttime the ion temperature is equal to the neutral temperature (Nisbet, 1967). Therefore, this temperature amplitude may be too high by about 10%.

All measurements collected in Table I are made during moderate solar activity ($F = 100 - 150$). For comparison we therefore selected model 4 of CIRA ($F = 125$) (dashed lines in Figures 1 and 2) and Jacchia's (1964) model at $F = 125$ (dash-dotted lines in Figures 1a and 2a). From comparison between the observed data (No. III to VI) with the models No. I and II we notice immediately that neither the CIRA model nor Jacchia's model are in agreement with the observed density variations below 200 km altitude.

The calculated values of our two dimensional model which are plotted as full lines in Figures 1 to 4 are the result of a solution which fits optimally to all available observed data. The agreement between observed temperature and density observations and our calculation is quite good (Figures 1 and 2).

Also the horizontal wind approaches rather close to the horizontal wind field at about 110 km height which was derived by Kato (1956) from the S_q variation on a rotating earth (see Figure 3). We compare the horizontal wind with calculations made by Kohl and King (1967) and Geisler (1967) who determined winds from the horizontal pressure gradients inherent in Jacchia's model (1964). Kohl and King's (1967) winds at the equator at 300 km altitude (see their Figure 6)

show a maximum westerly flow at $\tau_v = 21^{\text{00}}$ local time and a magnitude of $A_v = 140$ m/sec. Geisler (1967) obtains very similar numerical data. This is in reasonable agreement with our theoretical results in Figure 3 which give $A_v = 147$ m/sec and $\tau_v = 21^{\text{40}}$ local time.

Recently, Dickinson and Geisler (1968) evaluated the vertical velocity of the diurnal thermospheric tide from the static Jacchia model (1964). To do this, they integrated the equation of continuity, which preassumes an exact knowledge of the pressure field throughout the thermosphere as well as the boundary conditions at the lower boundary. Since the observed density structure is in disagreement with Jacchia's model below 200 km Dickinson and Geisler's vertical winds cannot be expected to be realistic. Never-the-less at 300 km altitude the magnitude of their vertical wind velocity is 4 m/sec which is only a factor of two larger than our value. The time of the velocity maximum in Dickinson and Geisler's meridional system is 16^{00} local time at 300 km compared with 10^{00} local time in our model.

5. THE "SECOND HEAT SOURCE"

In discussing energy transport we must distinguish clearly between the time average flux and its diurnal component. The time average of the energy flux carried by waves can be dissipated into heat of the surrounding air. This is an irreversible process which continuously heats the thermosphere and thus affects the time average thermosphere structures of density and temperature which are not discussed in this paper. The diurnal variation of the energy flux constitutes

a reversible process for waves which alternately changes from convective into conductive energy form and thus it affects the temporal variations in the thermosphere. It is this component of the diurnal wave that actually represents the "second heat source."

The way in which the diurnal wave alternatingly stores and drains energy is complex due to the various forms of energy transfer. In the energy equation [see Equation (2) of paper I] the temporal change of the internal energy is the result of the total heat input per unit volume and unit time

$$\rho c \frac{dT}{dt} = \Delta Q_{\text{total}} = \Delta Q_{\text{EUV}} + \Delta Q_{\text{HC}} + \Delta Q_{\text{EV}} \quad (14)$$

where ρ is the mean density, c is the specific heat at constant volume, ΔQ_{EUV} is the diurnal component of the EUV input,

$$\Delta Q_{\text{HC}} = \Delta Q_{\text{HC hor}} + \Delta Q_{\text{HC vert}} = -k_y^2 \kappa \Delta T + \frac{\partial}{\partial z} \left(\kappa \frac{\partial \Delta T}{\partial z} \right)$$

is the heat input due to heat conduction with its horizontal and vertical components, and

$$\Delta Q_{\text{CV}} = \Delta Q_{\text{CV hor}} + \Delta Q_{\text{CV vert}} = -j k_y p \Delta v - p \frac{\partial \Delta w}{\partial z}$$

is the heat input due to heat convection (or adiabatic heating) with its horizontal and vertical components.

To determine the relative importance of the various energy terms their magnitudes and phases have been calculated. They are plotted versus altitude in Figure 5. We have omitted $\Delta Q_{HC\text{ hor}}$, which is at least two orders of magnitude smaller than the other terms. We notice from Figure 5 that the heat inputs from horizontal and vertical heat convection are comparable with the heat input from the solar EUV radiation up to 300 km altitude. In this same altitude range vertical heat conduction is relatively insignificant while above 350 km this process becomes the dominating one.

From the input rates in Figure 5 it becomes immediately clear why the earlier models failed to describe the thermosphere consistently:

The Harris and Priester Model is one dimensional and thus does not consider the very significant contributions from horizontal heat convection. Due to the boundary conditions in this model, the contribution of vertical heat conduction at high altitudes and the contribution of vertical heat convection at 120 km were suppressed. In our model these processes are shown to be of dominating significance.

The two dimensional model of Volland (paper I) correctly predicts the significance of horizontal heat convection, but it fails to achieve quantitative agreement because it does not consider the very effective energy exchange through heat convection at 120 km.

What applies to the previous models basically also applies to the model of Dickinson et al.

To explain the origin of the "second heat source" we show in Figure 6 the various energy inputs that flow per unit time into a thermospheric column above unit area between 120 and 400 km height. These inputs are primarily due to EUV (note that in our representation only the first Fourier component is considered), vertical heat convection (which in our model results mainly from the large convective energy flow through 120 km), horizontal heat convection and vertical heat conduction. Harris and Priester assumed that horizontal heat convection is zero and that the corresponding input from vertical heat convection results only from a comparatively small convective energy flow at the upper boundary of their model. Therefore we can clearly identify the origin of their "second heat source". It results primarily from the convective energy transfer which is suppressed by their choice of boundary conditions and their restriction to one dimension. In our model this convective heating is induced by the EUV heat input and by a tidal wave generated below 120 km. We see from Figure 6 that both the horizontal and the vertical component of heat convection are each comparable with the EUV input, while their phases are shown to be significantly different from that of the EUV source.

Adding the two convective inputs we show our equivalent of the "second heat source", ΔQ_{sec} , in Figure 7 (solid line). As we see the maximum of ΔQ_{sec} occurs at 5° local time and its magnitude is $0.5 \text{ erg/cm}^2 \text{ sec}$. This maximum before noon shifts the total heat input into the morning hours thus shifting the maximum of temperature and density from the late to the early afternoon which is in agreement with observations. The first Fourier component of the "second heat source" of Harris and Priester (1963) is also shown in Figure 7 (dashed

line). As evident this source has about the same form as our convective heat input. The amplitudes of both heat inputs are almost identical. Harris and Priester's "second heat source" however peaks three hours later than ΔQ_{sec} , a discrepancy that is understandable if we consider that Harris and Priester did not describe the relatively large density and temperature variations in the lower thermosphere. These variations are in our model partly induced by vertical heat convection which — as we see from Figure 6 — peaks at 2⁰⁰ local time and thus is responsible for shifting in our model the convective heat input into the early morning.

Above 300 km altitude the diurnal tidal wave from the lower atmosphere has lost its predominant influence on the diurnal density variation. The "second heat source" at these heights is in our model due to the open boundary between thermosphere and exosphere which allows the upgoing characteristic waves to propagate freely into the exosphere. In the Harris-Priester model as well as in the Dickinson et al.-model the unrealistic upper boundary condition of zero temperature gradient gives rise to peculiar interferences between upgoing and downgoing waves at the upper boundary. This is analogous to a closed "wave guide" that confines the diurnal wave energies between two fixed boundaries, and thus causes the too large density variations in the calculations of Harris and Priester (1962) as well as of Dickinson et al. (1968).

6. CONCLUSION

A two dimensional model of the thermosphere between 120 and 400 km is presented in which the solar EUV heat input is the only external heat source

taken into account. This is in contrast to Harris and Priester's model in which additionally an unspecified "second heat source" was required.

In our model we successfully reproduced the amplitude and phase of the diurnal thermospheric density and temperature variations. The relative diurnal density variation is thereby shown to be significantly higher than the CIRA model predictions below 250 km in accordance with measurements by Spencer et al. (1966) and Taeusch et al. (1968). The horizontal wind field in our model agrees in phase and amplitude with the wind field derived from the S_q currents below 120 km (Kato, 1956), and it is also found to be consistent with the wind field derived from the Jacchia model (Kohl and King, 1967).

The main differences that characterizes our model when comparing it with the Harris-Priester model are the following:

1. Our model is two dimensional. Therefore we consider not only vertical convection but also horizontal convective energy flow which — as predicted in paper I — is of great significance. This energy flow is induced by the EUV heat input and intensified by heat convection due to a tidal wave propagating upward into the thermosphere. This tidal wave plays a dominating role up to 200 km and remains significant even above 300 km.

The effects of convective energy transport are twofold. Firstly, as we have shown in this paper, this process gives rise to energy inputs that are comparable with the input due to the diurnal EUV component. Yet the phase of the convective energy component is different from that of the EUV source. As a result, the convective energy transfer acts like

Harris and Priester's "second heat source" thus shifting the density and temperature maximum from the late afternoon into the early afternoon.

Secondly, in our model, it is the transport process of convection that

plays the major role in the energy balance of the lower thermosphere.

This is in contrast to Harris and Priester's model in which heat conduction predominates. Our emphasis on heat convection is necessarily

associated with enhanced mass transport and this increases the diurnal density amplitude over that in Harris and Priester's model below

250 km.

2. Energy exchange through vertical heat conduction is considered to play a major role at the upper boundary of our model at 400 km. There, relatively small variations of the heat flux and thus very small variations of the temperature gradient contribute significantly to the diurnal energy balance because of the small energy content at these heights.

This is in contrast to Harris and Priester's model in which heat conduction is suppressed through their choice of the upper boundary conditions.

In their model the diurnal energy exchange at the upper boundary was carried exclusively by heat convection. Therefore without their "second heat source" this convection was associated with mass exchange that resulted in density amplitudes much larger than are observed. With the "second heat source" their model of course described the density variations properly as it was introduced for this purpose.

ACKNOWLEDGMENT

We gratefully acknowledge critical and helpful comments from L. H. Brace.

LITERATURE

- CIRA, 1965: COSPAR international reference atmosphere. North Holland Publishing Company, Amsterdam
- Dalgarno, A., 1964: Ambipolar diffusion in the F-region. Journ. Atm. Terr. Phys. 26, 939
- Dickinson, R. E. and J. E. Geisler, 1968: Vertical motion in the middle thermosphere from satellite drag densities. Monthly Weather Rev., 96, 606-616
- Dickinson, R. E., Lagos, C. P. and R. E. Newell, 1968: Dynamics of the neutral gas in the thermosphere for small Rossby number motions. Journ. Geophys. Res., 73, 4299-4313
- Geisler, J. E., 1967: A numerical study of the wind system in the middle thermosphere. Journ. Atm. Terr. Phys., 29, 1469-1482
- Harris, I. and W. Priester, 1962: Time dependent structure of the upper atmosphere. J. Atm. Sci., 19, 286-301
- Harris, I. and W. Priester, 1963: Heating of the upper atmosphere, Space Research III, Amsterdam
- Harris, I. and W. Priester, 1965: Of the diurnal variation of the upper atmosphere. J. Atm. Sci., 22, 3-10
- Jacchia, L. G., 1964: Static diffusion models of the upper atmosphere with empirical temperature profiles. Special Report No. 170, Smithsonian Institution, Astrophysical Observatory, Cambridge, Mass.
- Kato, S., 1956: Horizontal wind systems in the ionospheric E region deduced from the dynamo theory of the geomagnetic S_q variation, Part II: rotating earth. J. Geomagn. Geoelectr., 8, 24-37

King-Hele, D. G. and J. Hingston, 1967: Variation in air density at heights near 150 km from the orbit of the satellite 1966-101G. *Planet. Space Sci.*, 15, 1883-1893

King-Hele, D. G. and J. Hingston, 1968: Air density at heights near 190 km from the orbit of SECOR 6. *Planet. Space Sci.*, 16, 675-691

Kohl, H. and J. W. King, 1967: Atmospheric winds between 100 and 700 km and their effects on the ionosphere. *Journ. Atm. Terr. Phys.*, 29, 1045-1062

Lindzen, R. S., 1967: Thermally driven diurnal tide in the atmosphere. *Quart. J. Roy. Meteorol. Soc.*, 93, 18-42

Mahajan, K. K., 1968: Diurnal variation of the ion temperature. *Journ. Atm. Terr. Phys.* (to be published)

Nisbet, J. S., 1967: Neutral atmospheric temperatures from incoherent scatter observation. *Journ. Atm. Sci.*, 24, 586-593

Taeusch, D. R., Niemann, H. B., Carignan, G. R., Smith, R. E. and J. O. Ballance, 1968: Diurnal survey of the thermosphere. I: Neutral particle results. Space Research VIII, p. 930-939, North Holland Publishing Company, Amsterdam

Spencer, N. W., D. R. Taeusch and G. R. Carignan, N₂ temperature and density data from the 150 to 300 km region and their implications, *Annales De Geophysique*, 22, 1966

Volland, H., 1966: A two dimensional dynamic model of the diurnal variation of the thermosphere. I: Theory. *J. Atmosph. Sci.*, 23, 799-807

Volland, H., 1967: On the dynamics of the upper atmosphere. Space Research VII, p. 1193-1203, North Holland Publishing Company, Amsterdam

Volland, H., 1968: A theory of thermospheric dynamics. Part I: Diurnal and solar cycle variations. NASA Document X-612-68-503, GSFC, Greenbelt, Md.

Volland, H., 1969: The upper atmosphere as a multiply refractive medium for neutral air motions. Journ. Atm. Terr. Phys. (to be published)

Volland, H. and H. G. Mayr, 1969: The significance of the wave picture in the theory of diurnal tides within the thermosphere. NASA Document X-612-68-503, submitted to Journ. Geophys. Res.

Table I: List of authors the data of which have been used
for comparison with the theoretical model.

No.	Source	Observed or Derived Physical Parameter	Height Range	Method
I	CIRA (1965)	Density, Temperature	120-400	Model 4 (F = 125)
II	Jacchia (1964)	Density, Temperature	120-400	Model (F = 125)
III	Spencer et al. (1966)	Density, Temperature	150-300	Rocket
IV	Taeusch et al. (1968)	Density, Temperature	150-300	Rocket
V	King-Hele et al. (1967), (1968)	Density	155-190	Satellite Drag
VI	Mahajan (1968)	Temperature	250	Backscatter
VII	Kato (1956)	Horizontal Wind	110	Geomagnetic S_q current

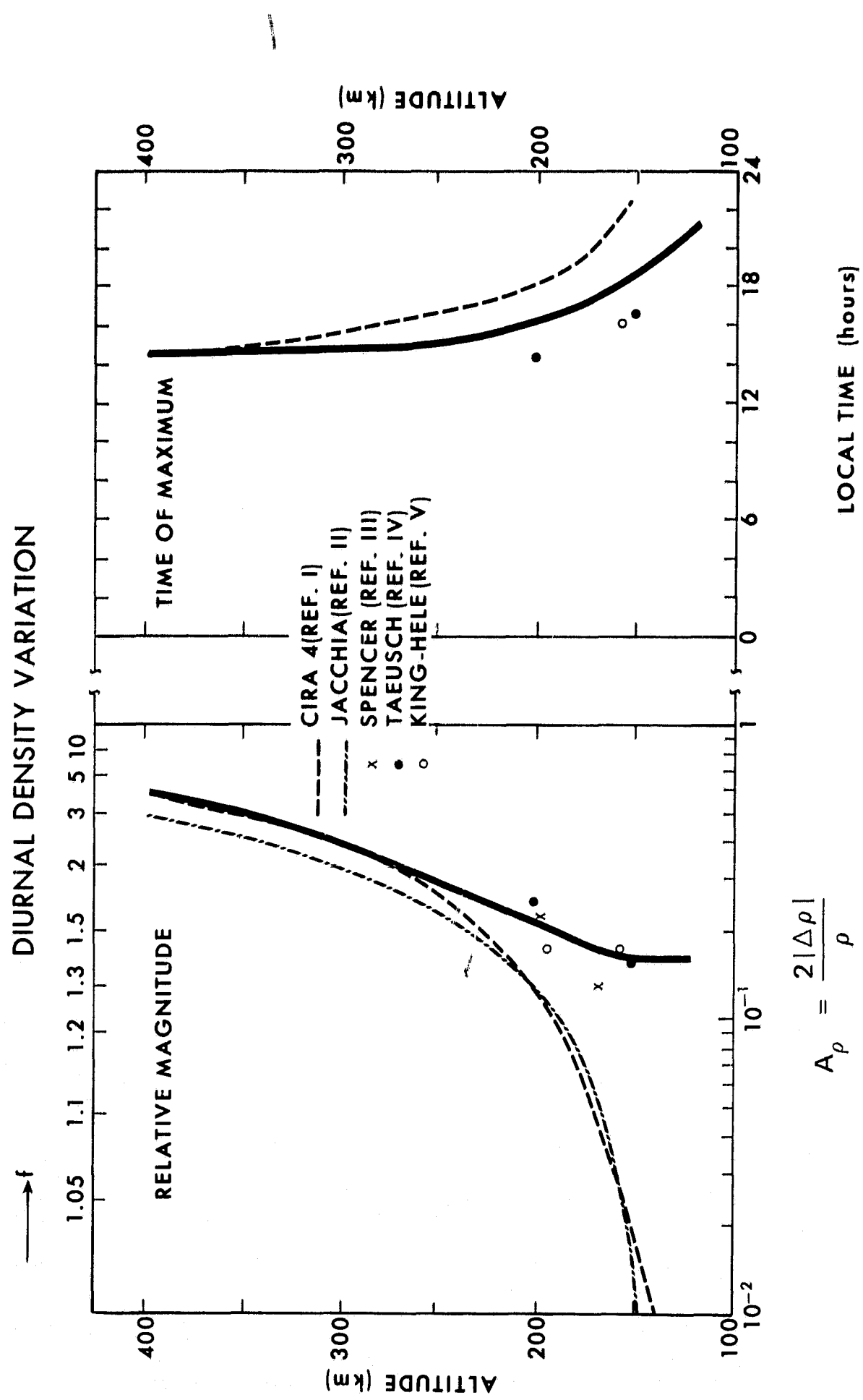


Figure 1. Diurnal density variation versus height. Full lines: two dimensional model; dashed lines: CIRA model 4; dash-dotted line: Jacchia model ($F = 125$); a. relative magnitude $A = \frac{2|\Delta\rho|}{\rho}$ b. time of maximum τ .

$$A_\rho = \frac{2|\Delta\rho|}{\rho}$$

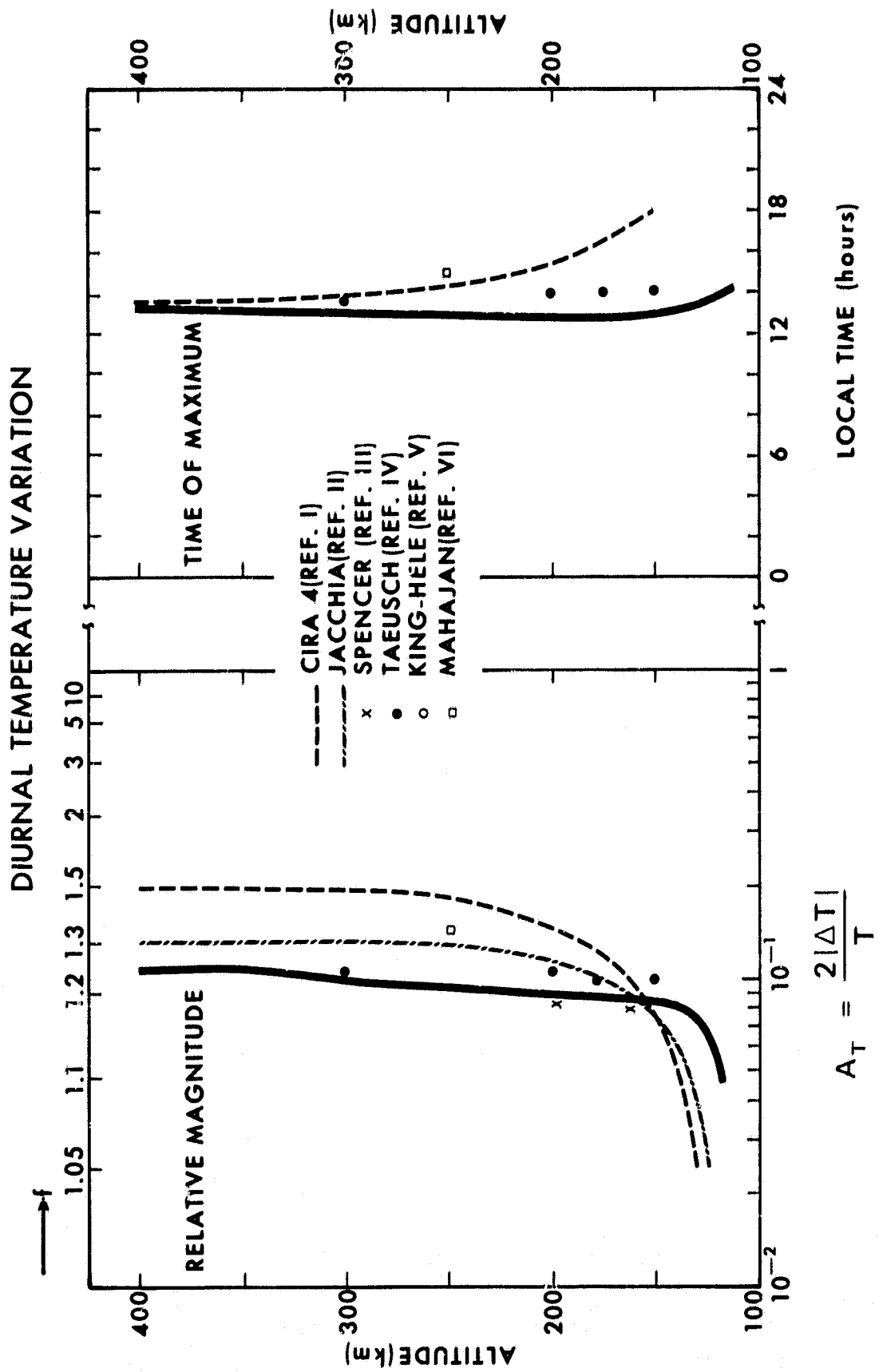


Figure 2. Diurnal temperature variation versus height. Full lines: two dimensional model; dashed lines: CIRA model 4; dash-dotted line: Jacchia model ($F = 125$); a. relative magnitude $A = \frac{2 |\Delta T|}{T}$; b. time of maximum τ .

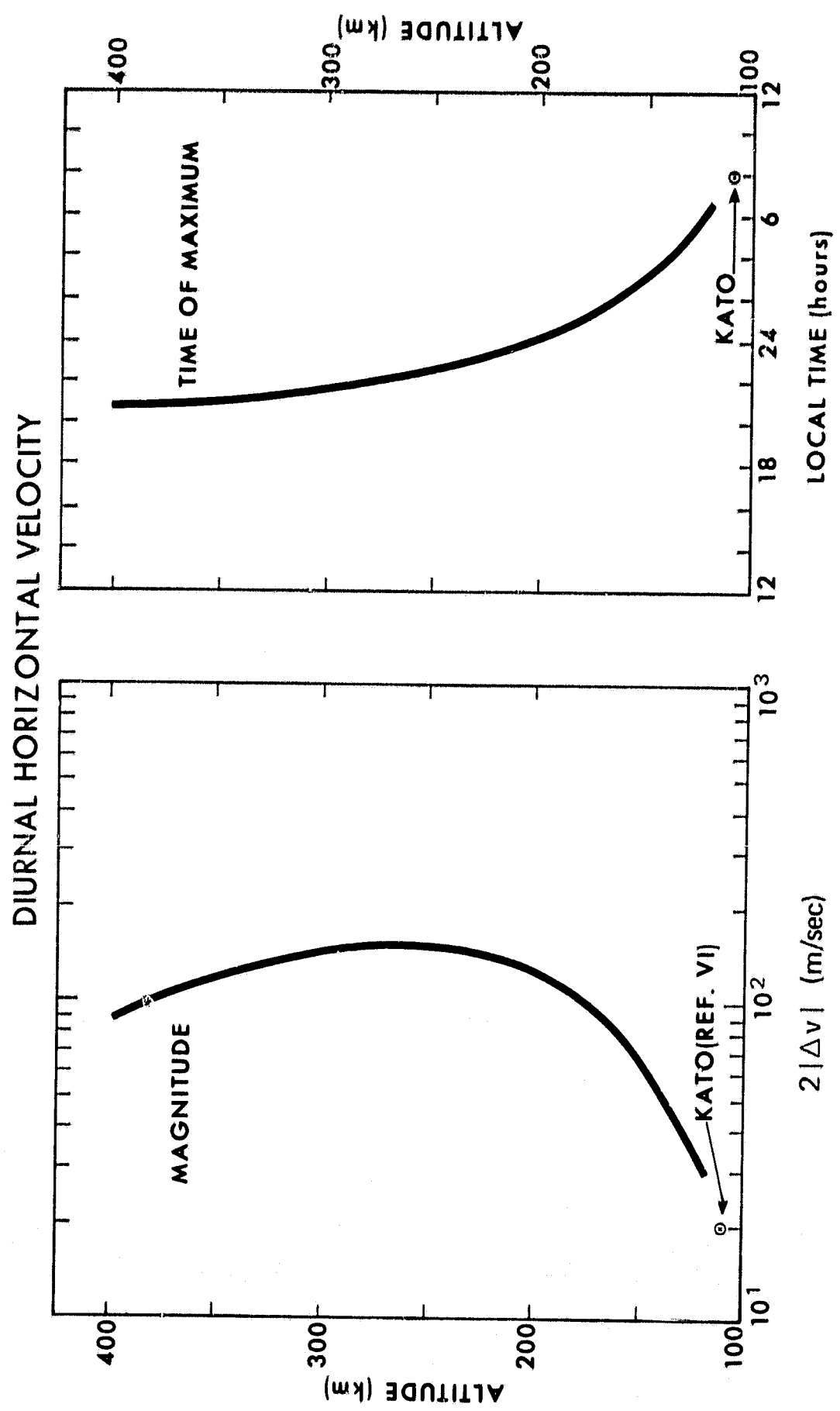


Figure 3. Diurnal variation of horizontal latitudinal velocity versus height (positive in eastern direction).

a. Magnitude $A = 2 |\Delta v|$ (m/sec). b. Time of maximum T .

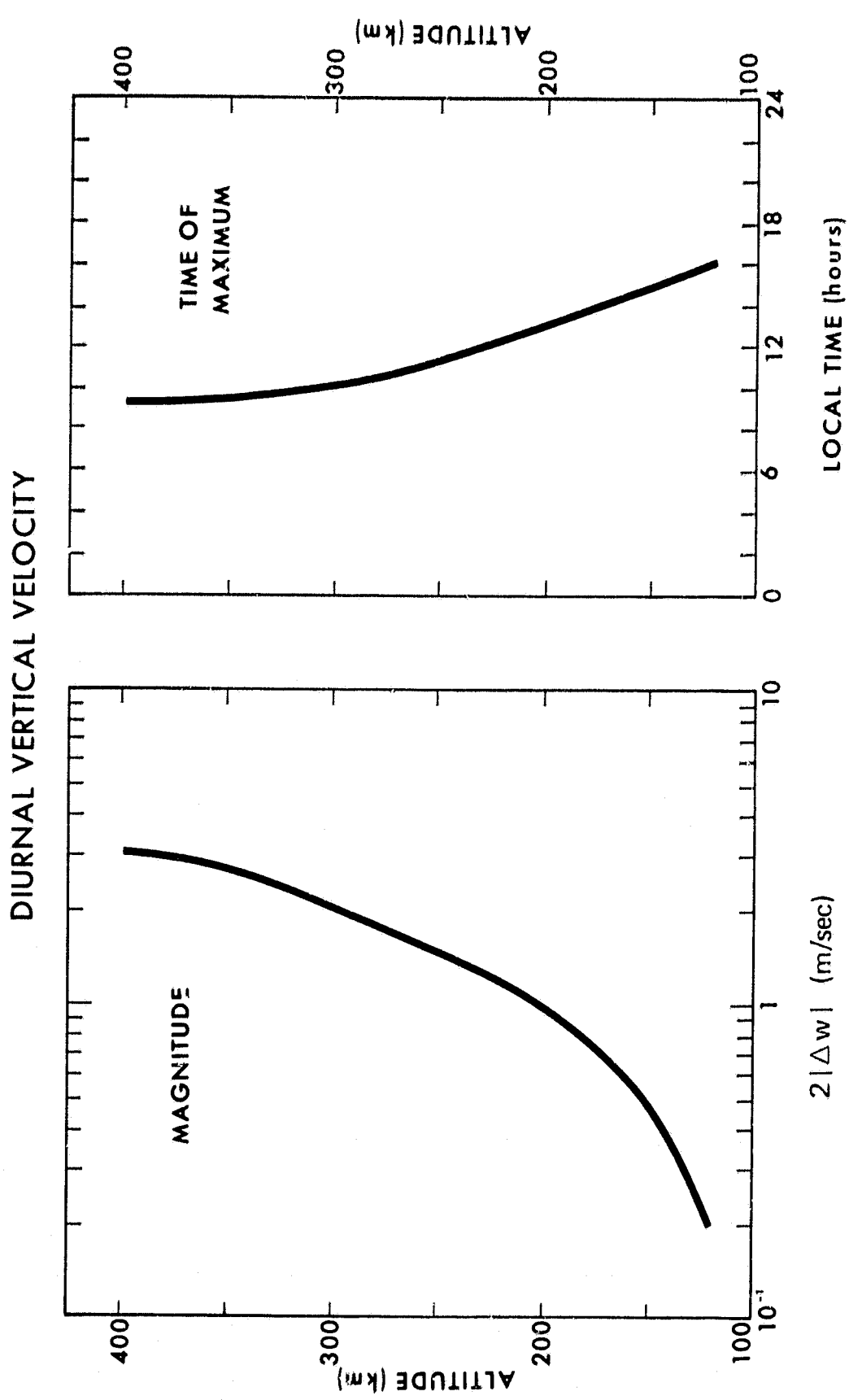


Figure 4. Diurnal variation of vertical velocity versus height. a. Magnitude $A = 2 |\Delta w|$ (m/sec). b. Time of maximum τ .

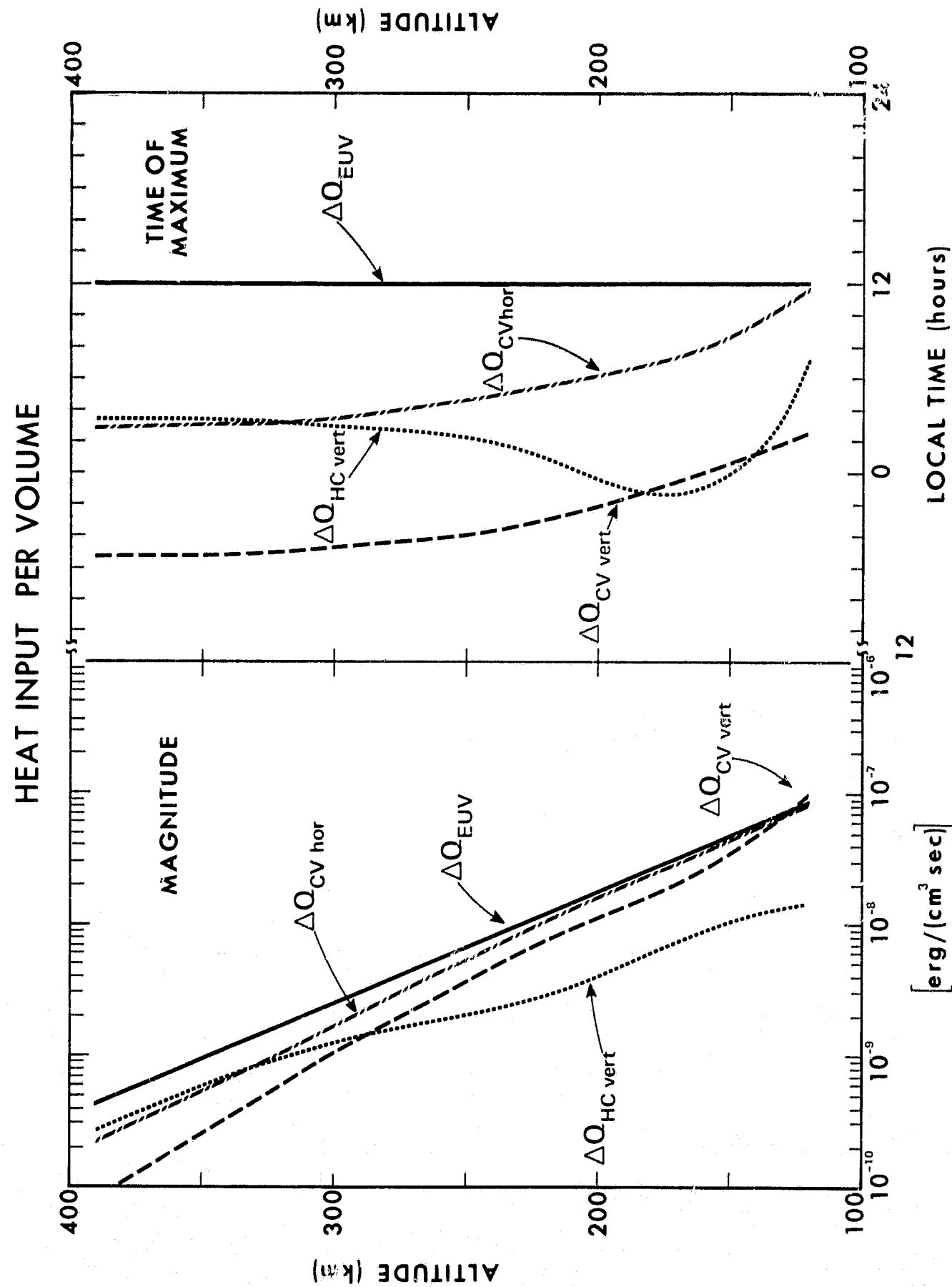


Figure 5. Heat input per volume and time within the thermosphere due to EUV and due to heat conduction and heat convection of the diurnal wave. a. Magnitude. b. Time of maximum heating.

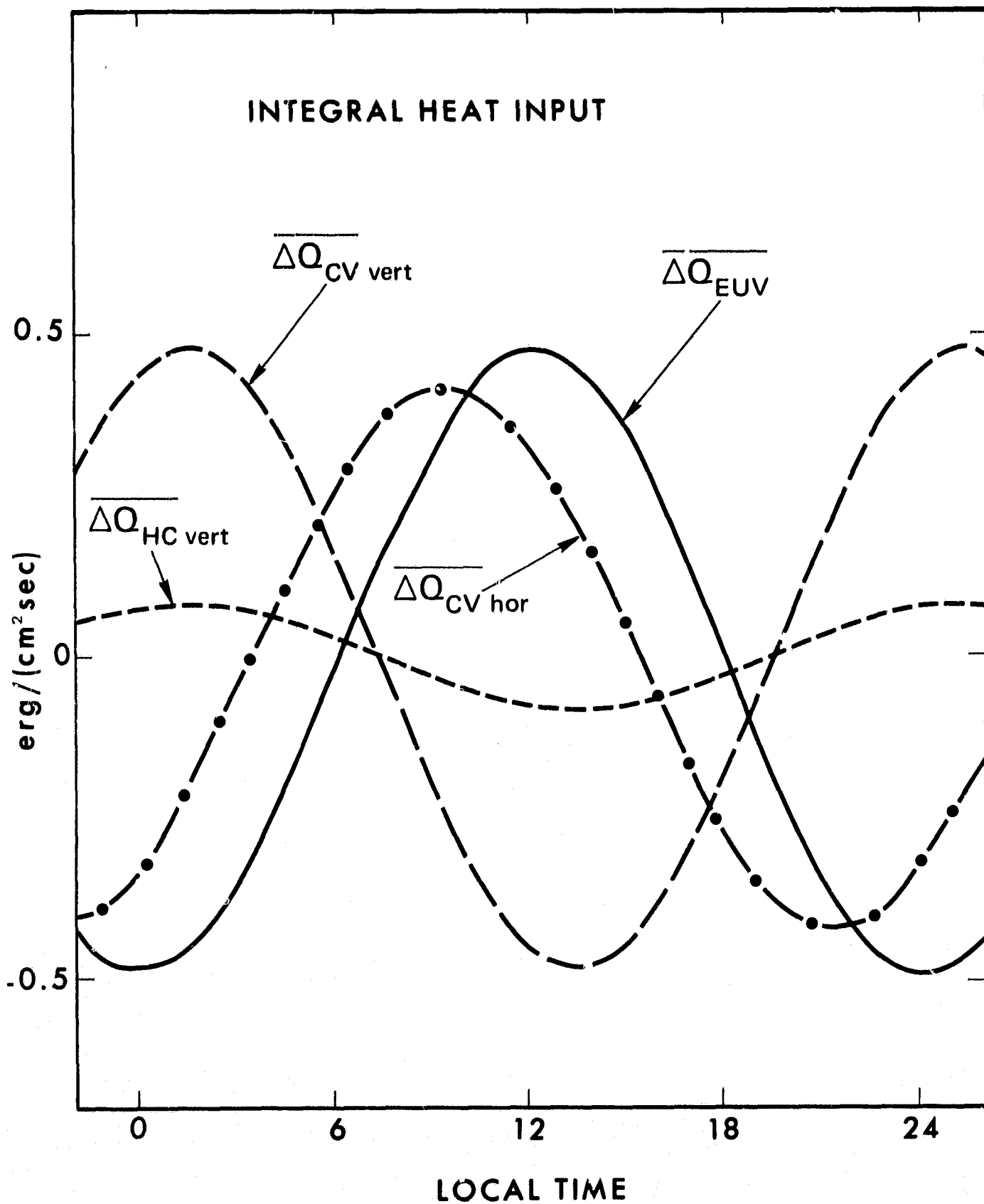


Figure 6. Integral heat input within a unit column of the thermosphere due to the diurnal component of EUV, to heat conduction and heat convection of the diurnal wave versus local time.

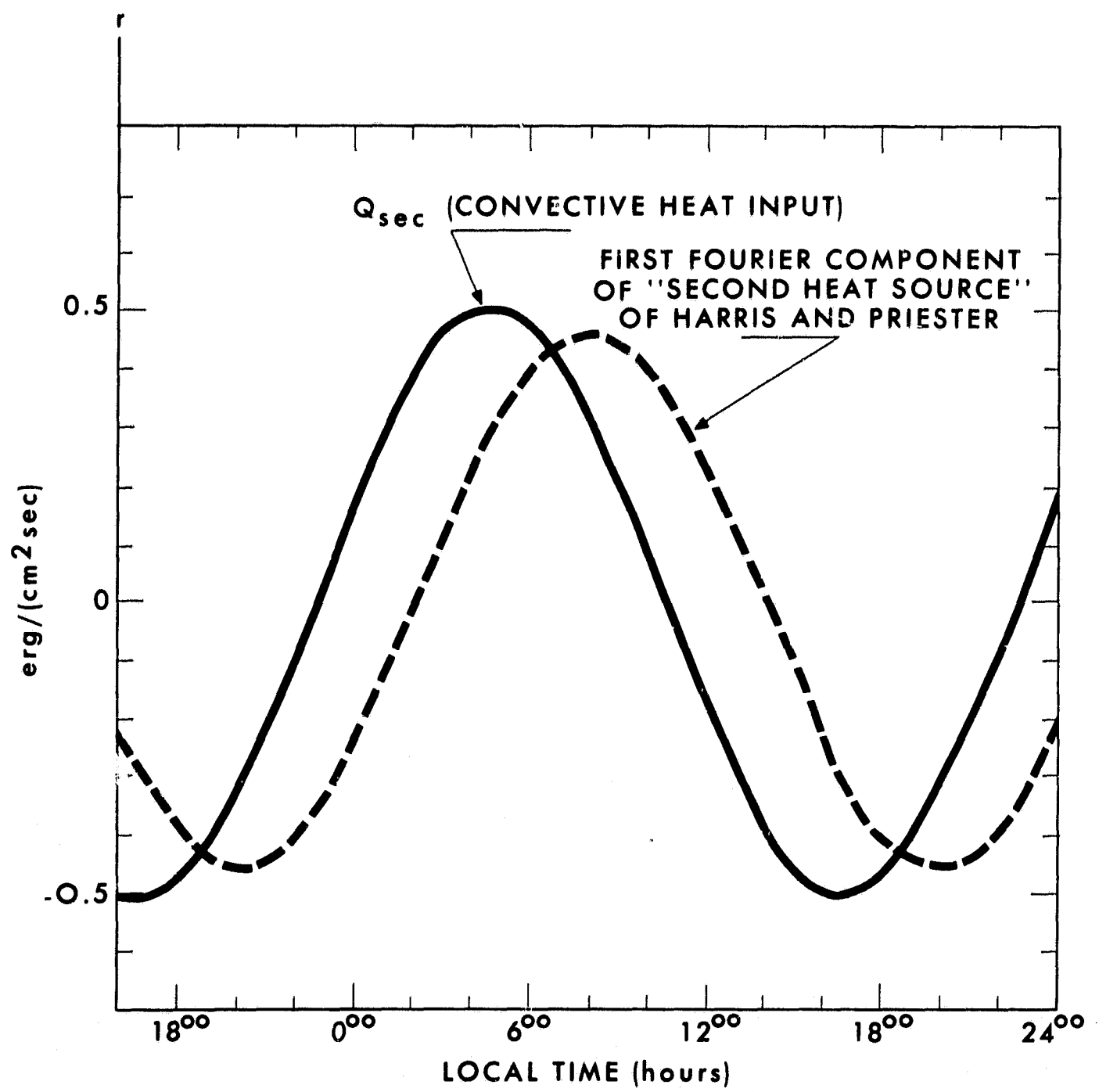


Figure 7. Integral convective heat input, equivalent to a second heat source, $\Delta Q_{sec} = \Delta Q_{CV}$ and first Fourier component of "second heat source" of Harris and Priester (1963).